



HAL
open science

Effects of soil foundation on the performance of masonry buildings

Fernando Lopez-caballero, Arézou Modaresi-Farahmand Razavi, Maryam Tabbakhha

► To cite this version:

Fernando Lopez-caballero, Arézou Modaresi-Farahmand Razavi, Maryam Tabbakhha. Effects of soil foundation on the performance of masonry buildings. 8th International Conference on Structural Dynamics, EURODDN 2011, Jul 2011, Leuven, Belgium. pp.185-191. hal-04603193

HAL Id: hal-04603193

<https://hal.science/hal-04603193v1>

Submitted on 6 Jun 2024

HAL is a multi-disciplinary open access archive for the deposit and dissemination of scientific research documents, whether they are published or not. The documents may come from teaching and research institutions in France or abroad, or from public or private research centers.

L'archive ouverte pluridisciplinaire **HAL**, est destinée au dépôt et à la diffusion de documents scientifiques de niveau recherche, publiés ou non, émanant des établissements d'enseignement et de recherche français ou étrangers, des laboratoires publics ou privés.

Effects of soil foundation on the performance of masonry buildings

F. Lopez-Caballero¹, A. Modaressi-Farahmand-Razavi¹, M. Tabbakhha¹

¹Laboratoire MSS-Mat CNRS UMR 8579, Ecole Centrale Paris, France

email: : fernando.lopez-caballero@ecp.fr, arezou.modaressi@ecp.fr, maryam.tabbakhha@ecp.fr

ABSTRACT: The present paper deals with the influence of soil non-linearity, on the soil- foundation-structure interaction phenomena. Numerical simulations are carried out so as to reveal the beneficial or unfavourable effects of the non-linear SSI on the assessing of damages of masonry structures. The importance of input earthquake characteristics on the structural damages in the masonry structure is evaluated through a numerical probabilistic analysis. The influence of the inelastic behaviour of soil deposit on the amplification of ground seismic accelerations and on the soil-interaction effects is highlighted.

KEY WORDS: Seismic fragility; Dynamic soil-structure interaction; Inelastic behaviour; Masonry.

1 INTRODUCTION

The aim of this work is to assess numerically the role of the non-linear soil behaviour on the seismic response of masonry structures founded on a rigid shallow foundation. In common practice of earthquake engineering, some simplified procedures take account of dynamics soil-structure interaction (SSI) effects on the determination of the design earthquake forces and the corresponding displacements via kinematics and foundation damping effects. All these procedures are based in traditional SSI expressions with linear-elastic soil behaviour assumption [1], [2], [3].

For this purpose, a model to represent a two-story masonry structure is selected and the influence of non-linear SSI on its seismic damage assessment is studied. Thus several 2D finite element computations are carried out using a realistic non-linear elastoplastic model to represent the soil behaviour [4], [5] in the numerical *GEFDyn* code [6]. A diagonal strut model using the plastic concentrator approach represents the behaviour of the masonry panels and a continuous non-linear beam model is used to represent the structural elements' behaviour.

It is well known that the ground response depends on both the material properties of soil profile and the outcropping input motion. Thus, several nonlinear dynamic analyses are performed in order to evaluate the role of different parameters on the seismic response.

A numerical probabilistic analysis is performed so as to quantify both the impact of the uncertainties associated with the input signal and the effect of the SSI on the structural damage in the masonry structure. The response in terms of top displacement was calculated and used to construct fragility curves. This kind of curves give the probability of exceeding different levels of damage, with respect to the earthquake intensity. In order to quantify the beneficial or unfavourable effects of the non-linear SSI on the induced damage in the masonry the computed fragility curves with and without SSI effects are compared.

2 NUMERICAL MODEL

For the purpose of studying the effect of soil foundation on the structural response, a layered soil/rock model is considered (figure 1(a)). The soil profile is composed principally of medium dense sand. The total thickness of the soil profile is 30m over the bedrock. The shear wave velocity of the soil increases with depth and the shear wave velocity profile gives an average shear wave velocity in the upper 30m (V_{s30}) of 243m/s, corresponding to a category C site of Eurocode8.

2D finite elements computations with a modified plane-strain approach [7] for the soil are performed. The soil is modelled using quadrilateral isoparametric elements with four nodes. The element integration of the soil is 2×2 full Gauss-integration. The thicknesses of the soil plane-strain elements is 4m. An implicit Newmark numerical integration scheme with $\gamma = 0.625$ and $\beta = 0.375$ is used in the dynamic analysis [8].

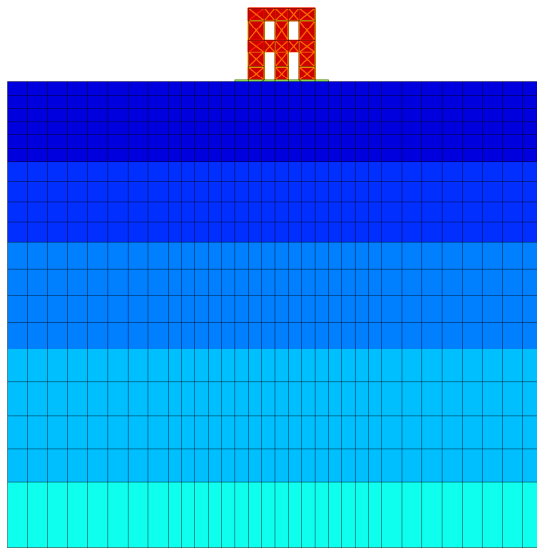
In the SSI analysis, only vertically incident shear waves are introduced into the domain and as the response of an infinite semi-space is modelled, equivalent boundaries have been imposed on the nodes of lateral boundaries (i.e. the normal stress on these boundaries remains constant and the displacements of nodes at the same depth in two opposite lateral boundaries are the same in all directions).

For the bedrock's boundary condition, paraxial elements simulating a "deformable unbounded elastic bedrock" have been used [9]. The incident waves, defined at the outcropping bedrock are introduced into the base of the model after deconvolution. Thus, the obtained movement at the bedrock is composed of the incident waves and the reflected signal.

2.1 Structural model

A scheme of the two-story masonry building chosen to represent the structure is given in figure 1(b). The total height of the building is 5.4m, the width is 5.0m and the thicknesses is 0.16m. With these characteristics the fundamental period of the structure (T_{str}) is equal to 0.19s. This structure is modelled using three different kinds of elements, beam-columns and diagonal

struts describing the structural behaviour and strengthless solid elements to represent the masonry mass.



(a)

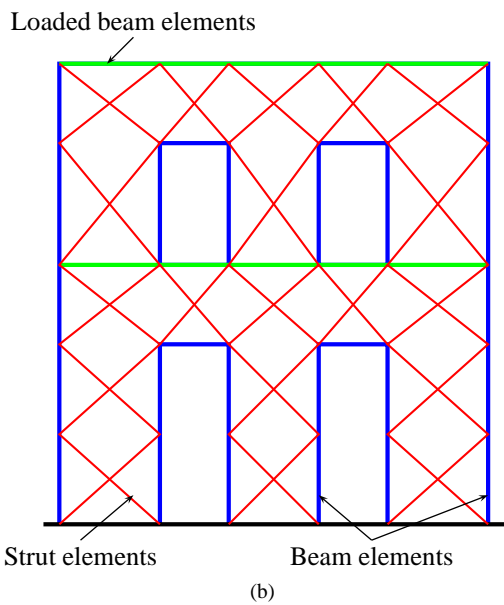


Figure 1. a) Finite element mesh for SSI approach and b) Building scheme.

The frame's structural elements are modelled by plastic hinge beam-column elements. The model is based on the two-component model presented by [10] and the modifications introduced by [11] to take into account axial force and bending moment interaction. In this work, the behaviour of the masonry is simulated by a model based on the theory of plasticity and the concept of an equivalent strut. The masonry panel is simulated as one element conformed by two diagonal struts of four nodes [12]. In order to include some coupling between the two struts the displacements at the top of each one are equivalent. An elastic-plastic model with stiffness degradation for strut behaviour is considered [13].

In order to verify the selected model parameters, a $1.6 \times 1.6m$ RC frame with an infill panel subjected to monotonic and cyclic loadings was simulated. The section of the plastic hinge beams is $13 \times 16cm$. The obtained shear base force (V) and top displacement (u_{top}) curves for the monotonic and cyclic loadings are displayed in figure 2.

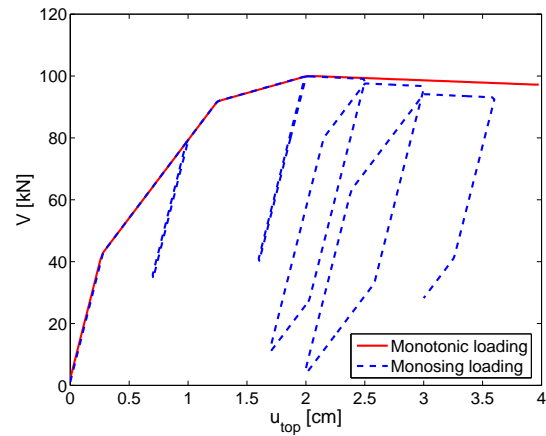


Figure 2. Numerical simulation of shear base force (V) and top displacement (u_{top}) curve in an infilled frame under monotonic and cyclic monosign loadings.

2.2 Soil model

The elastoplastic multi-mechanism model developed at *École Centrale Paris*, known as ECP model [4], [5] is used to represent the soil behaviour. This model can take into account the soil behaviour in a large range of deformations. The model is written in terms of effective stress. The representation of all irreversible phenomena is made by four coupled elementary plastic mechanisms: three plane-strain deviatoric plastic deformation mechanisms in three orthogonal planes and an isotropic one. The model uses a Coulomb type failure criterion and the critical state concept. The evolution of hardening is based on the plastic strain (deviatoric and volumetric strain for the deviatoric mechanisms and volumetric strain for the isotropic one). To take into account the cyclic behaviour a kinematical hardening based on the state variables at the last load reversal is used. The soil behaviour is decomposed into pseudo-elastic, hysteretic and mobilized domains. Refer to [4], [5], [14] among others for further details about the ECP model.

The $G/G_{max} - \gamma$ and $D - \gamma$ curves generated by the model simulations are shown in figure 3. The tests results are compared with the reference curves given by [15].

2.3 Input earthquake motion

In order to define appropriate input motions to the non-linear dynamical analysis, a selection of recorded accelerograms are used. The adopted earthquake signals are proposed by [16], [17], [18], [19]. Thus, 282 unscaled records were chosen from the Pacific Earthquake Engineering Research Center (PEER) database. The events range between 5.2 and 7.6 in magnitude and the recordings have site-to-source distances from 15 to

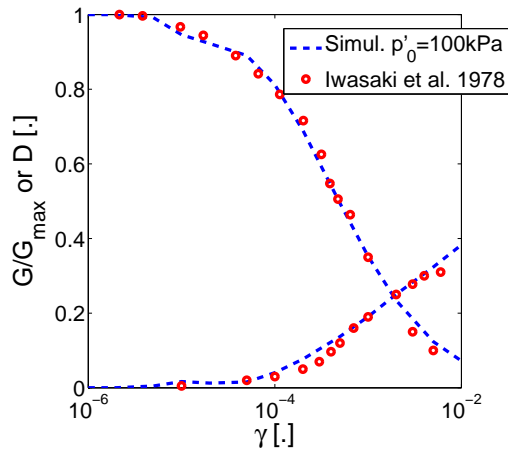


Figure 3. Comparison between simulated and reference $G/G_{max} - \gamma$ and $D - \gamma$ curves obtained by [15].

50km and dense-to-firm soil conditions (i.e. $360m/s < V_{s30m} < 800m/s$).

Concerning the response spectra of input earthquake motions, figure 4 shows the mean and the response spectra curves with a probability of exceedance (PE) between 2.75 and 97.5%. It can be noted that the mean response spectra is consistent with the response spectra of Type A soil of Eurocode8 scaled to the mean outcropping a_{max} value.

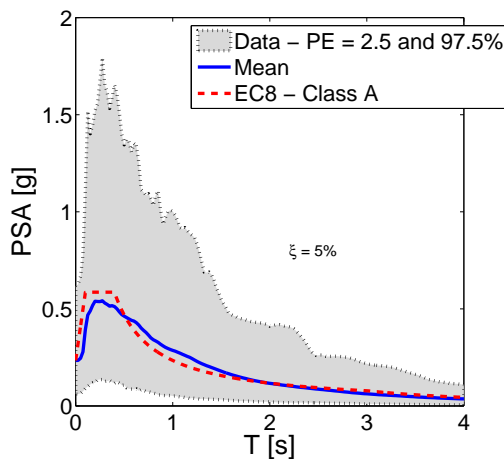


Figure 4. Response spectra of input earthquake motions.

The statistics on some input earthquake characteristics obtained for the strong ground motions are summarized in Table 1. These earthquake characteristics are maximal outcropping acceleration (a_{max}), Arias intensity (I_{Arias}) [20], predominant period (T_p), mean period (T_m) [21], period of equivalent harmonic wave ($T_{V/A} = \alpha \cdot pgv/pgv_a$), spectral acceleration at the first-mode period of the structure ($Sa_{T=0.2s}$), spectral intensity (SI), peak ground velocity (pgv), root-mean-square intensity (I_{rms}) [22], Cosenza and Manfredi dimensionless index (I_D) [23] and the significant duration ($t_{5\ 95}$).

Table 1. Statistics characteristics for the selected earthquakes

Parameter	Range	Mean	CV[%]
a_{max} [g]	0.03 – 0.88	0.23	67
T_m [s]	0.22 – 1.46	0.63	36
T_p [s]	0.10 – 1.15	0.38	58
$T_{V/A}$ [s]	0.16 – 1.43	0.55	40
I_{Arias} [m/s]	0.02 – 7.30	0.91	125
$t_{5\ 95}$ [s]	2.90 – 62.13	15.84	57
I_{rms} [m/s ²]	0.05 – 1.75	0.33	68
pgv [m/s]	0.03 – 1.66	0.25	78
I_D [-]	2.05 – 29.87	9.16	50
SI [m]	0.12 – 4.60	0.90	75

3 RESPONSE ANALYSIS

3.1 Soil ground response

Regarding the acceleration history obtained at the free field in our analyses, figure 5 shows the variation of peak ground acceleration at the surface ($a_{max\ FF}$) as a function of the maximum acceleration at the outcropping bedrock ($a_{max\ out}$). According to this figure, the amplification of peak ground acceleration on the ground surface relative to bedrock appears before $a_{max\ out}$ value equal to 0.6g. It is also interesting to note that, as expected, an amplification factor equal to 2 is found.

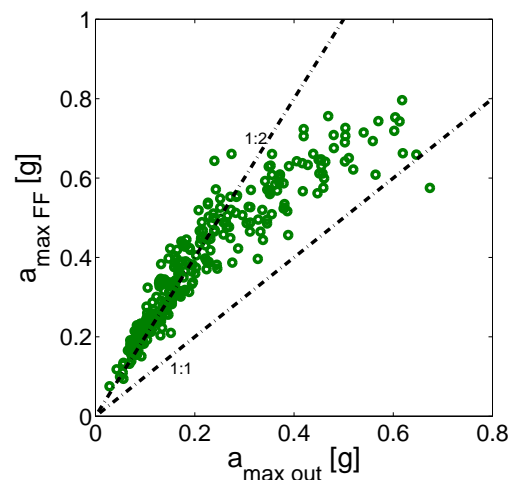


Figure 5. Relationships between maximum accelerations on bedrock ($a_{max\ out}$) and free field ($a_{max\ FF}$) obtained for the soil profile.

Concerning the frequency content of the surface signal, figure 6(a) shows the mean and the surface response spectra curves with a probability of exceedance (PE) between 2.75 and 97.5%. The mean response spectra of outcropping signals is superposed in the same figure as reference. A comparison of mean surface and outcropping normalized response spectra is given in figure 6(b). As expected, due to soil softening, for periods larger than about 0.5s, mean spectral surface accelerations are greater than the mean outcropping ones. From the same figure, it can be also seen, that the mean response spectra obtained shifts to higher period values.

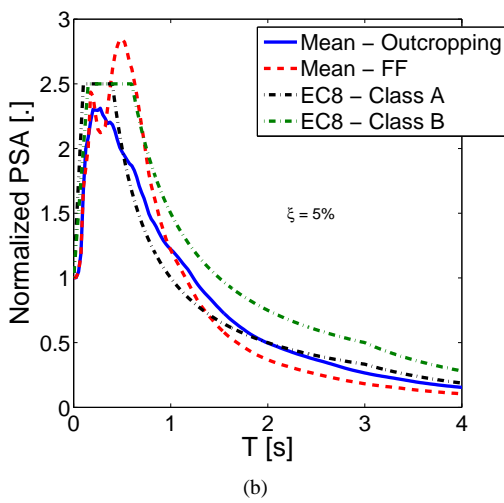
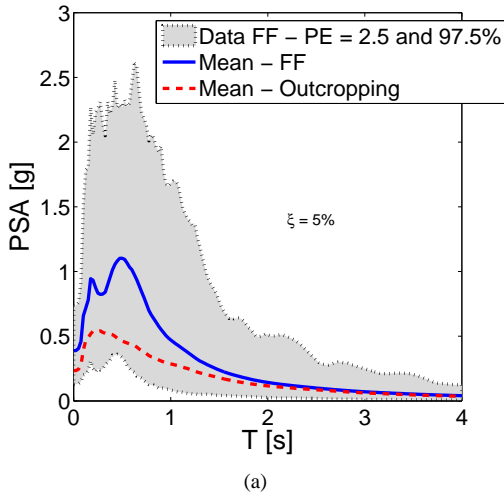


Figure 6. a) Response spectra of surface earthquake motions and b) Comparison of mean surface and outcropping normalized response spectra.

3.2 Seismic structural response

As proposed by [24], for the purpose of assessing the effect of inelastic *SSI* on the structure’s response, a comparative dynamical analysis is performed. In the first approach, the problem is decoupled. Firstly, an inelastic 1D wave propagation problem is solved for a simple soil column of the foundation soil. Then, the obtained free field motion is imposed as ground motion to a fixed base structural model. On the contrary, for the second approach, a complete finite element model including soil and structural inelastic behaviour is carried-out. Thus, the first approach takes into account non-linear behaviour of soil and superstructure, but neglects all interaction effects.

So as to define the structural reference case, the dynamic responses obtained by the masonry building model in fixed base condition are analysed. With regard to seismic demand evaluation on the building, the maximum top displacement (u_{top}) and its corresponding base shear force (V) observed during the dynamic computation are presented in figure 7. This curve corresponds to the dynamic capacity curve of the masonry building.

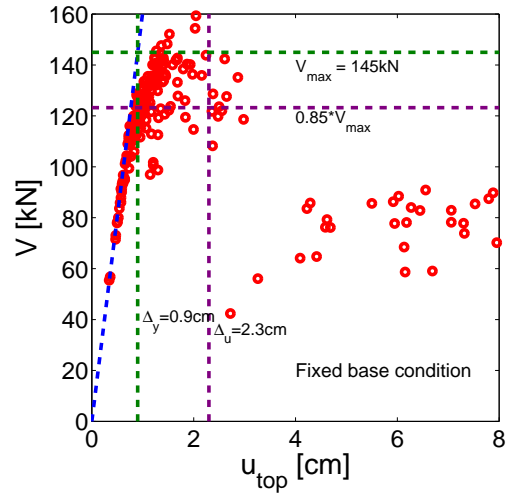


Figure 7. Structural dynamic response obtained for the masonry building at fixed base condition.

According to this figure, it is noted that a structural non-linear behaviour appears when $u_{top} > 0.9\text{cm}$, thus, this is the displacement corresponding to the yield capacity of the structure (Δ_y). The ultimate displacement of masonry building (Δ_u) is defined at 2.3cm (i.e. the maximum drift is equal to 0.4%).

In order to study the influence of the inelastic *SSI* on the structure’s response, a scatter plot comparing the maximum top displacement obtained in fixe base condition ($u_{top BR}$) with the relative top displacement obtained in *SSI* condition ($u_{top SSI}$) for the same outcropping motion is shown in figure 8. It is noted that for the majority of cases the top displacement decreases if the *SSI* is taken into account.

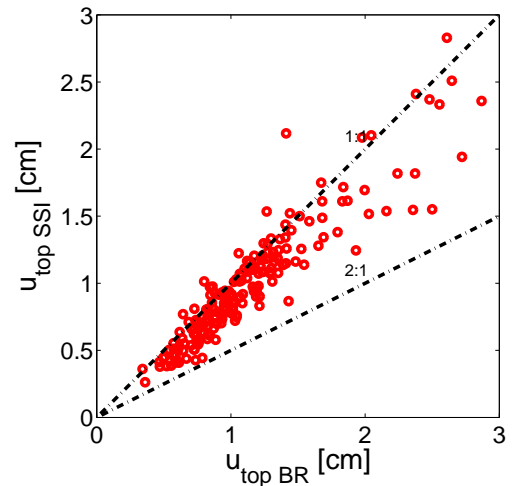


Figure 8. Comparison of relative top displacement obtained in *SSI* condition ($u_{top SSI}$) and in fixed base condition ($u_{top BR}$).

4 VULNERABILITY ANALYSIS

It is well known that fragility functions are an appropriate methodology for loss estimation purposes. They permit to represent a continuous potential damage for several discrete

damage levels and they give a probability of exceedance of these levels as a function of a seismic severity parameter. On this issue, to quantify the structural damage, the relative displacement between the top and the base of structure will be used. So as to use a common reference input value for different type of computations, we use motion's severity measures at outcropping.

According to a principal component analysis of obtained data, it is found that the variable u_{top} is well correlated with a_{max} and I_{Arias} . The obtained correlation coefficients are : $\hat{\rho}_{u_{top},a_{max}} = 0.81$ and $\hat{\rho}_{u_{top},I_{Arias}} = 0.78$ (figure 9(a)). Now, in order to confirm the influence of each earthquake parameter as well as to remove the co-variates on the correlation between a given input variable and the output variable, a sensitivity analysis based on the partial correlation coefficients (*PCC*) has been performed [25], [26]. The resulting *PCC* values between earthquake parameters and the output u_{top} variable can be seen in figure 9(b). As stated by these analyses, a_{max} is the most influential input variable on the structural drift. According to these figures, it is noted also that the structure's base condition does not affect this influence.

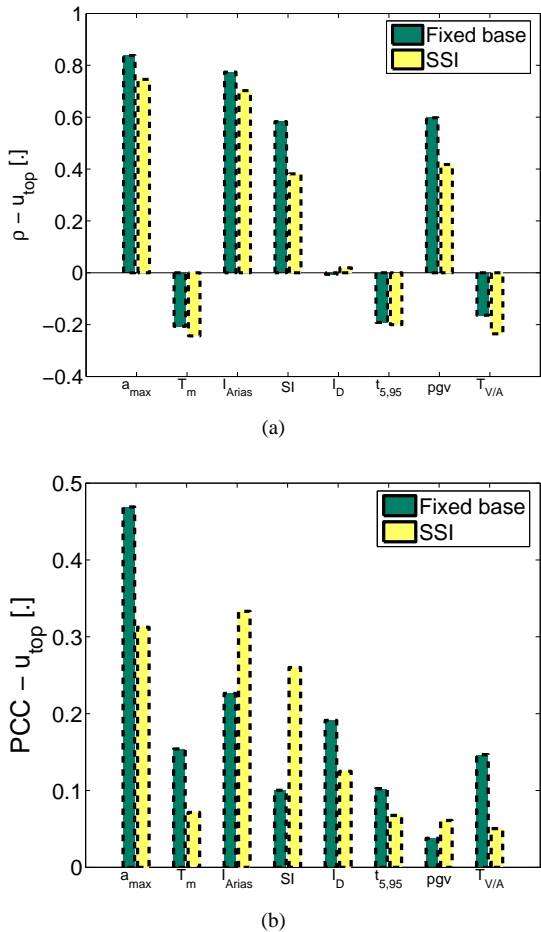


Figure 9. a) Correlation coefficients and b) Partial correlation coefficients of input random variables explaining u_{top} value.

Figure 10 provides the variation of u_{top} value with both maximal outcropping acceleration ($a_{max out}$) and Arias intensity ($I_{Arias out}$) for the fixed base condition. Referring to figure 10(a), it can be seen that as expected, the u_{top} value increases with an

increase in $a_{max out}$ value. It appears that $a_{max out}$ value provides a good correlation with the structure's damage.

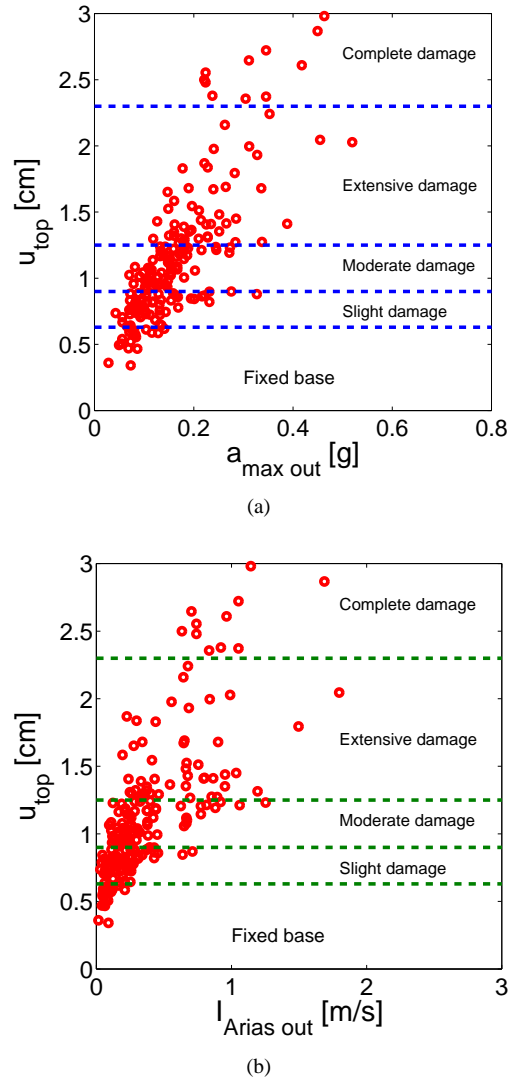


Figure 10. Scatter plot of top displacement (u_{top}) at fixed base condition as a function of a) maximal outcropping acceleration ($a_{max out}$) and b) Arias intensity ($I_{Arias out}$).

In this work, the fragility curves are constructed following the methodology proposed by [27], i.e. the maximum likelihood method is used to compute numerical values of the estimators $\hat{\alpha}$ and $\hat{\beta}$ of Log-normal distribution.

The damage states limits or the performance levels of the masonry building are those proposed by [28] and summarized in table 2. The four damage levels chosen are superposed in figure 10. They correspond to $u_{top} = 0.65, 0.9, 1.25$ and $2.3cm$. Figure 11 presents fitted fragility functions obtained for these three damage levels with respect to both $a_{max out}$ (figure 11(a)) and $I_{Arias out}$ (figure 11(b)) for the case with fixed base condition.

The statistical confidence of the derived fragility curves are superposed in figure 11(a) and figure 11(b) (dashed curves i.e. $\{\hat{\alpha}, \hat{\beta}\} \pm \{\sigma_1, \sigma_2\}$). This confidence is a function of the information provided by the size of motion database over the parameters $\hat{\alpha}$ and $\hat{\beta}$ describing the shape of each curve and it is computed via the Fisher information matrix [24]. Refer to [24]

among others for further details about the Fisher information matrix.

Table 2. Displacement limit states adopted from [28]

Damage state	Displacement threshold	Displacement value [cm]
Slight	$0.7 \cdot \Delta_y$	0.63
Moderate	Δ_y	0.90
Extensive	$\Delta_y + 0.25 \cdot (\Delta_u - \Delta_y)$	1.25
Complete	Δ_u	2.3

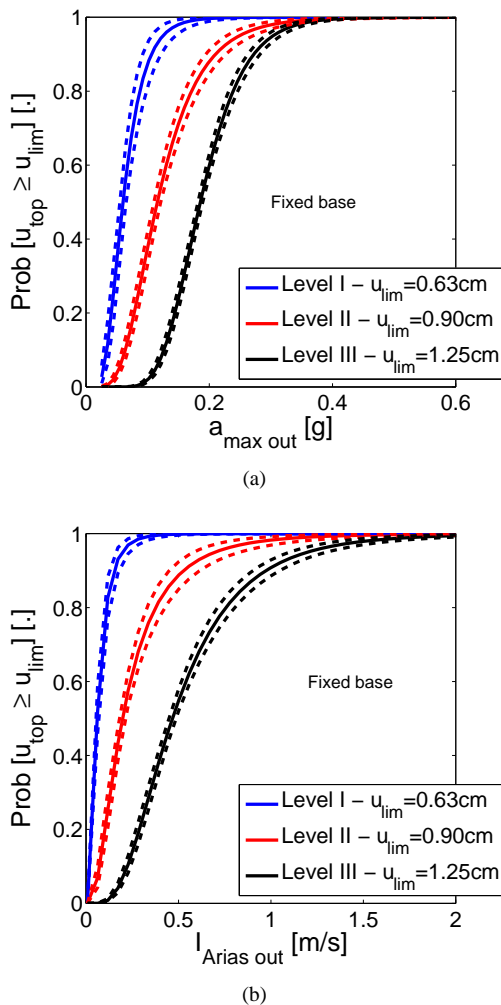


Figure 11. Fragility functions for three damage levels at fixed base condition. a) maximal outcropping acceleration ($a_{max out}$) and b) Arias intensity ($I_{Arias out}$).

Now, the effect of the inelastic SSI on the fragility functions obtained for two damage levels is studied. A comparison of the curves obtained for to structure’s base condition is displayed in figure 12. This comparison is done for two damage levels (i.e. Moderate and Extensive) with respect to $a_{max out}$. According to this comparison, it is noted that the fragility curves obtained shift to higher acceleration values for both damage levels when a fully inelastic SSI analysis is adopted. It means that for the

same $a_{max out}$ input value a lower probability of exceedance is found.

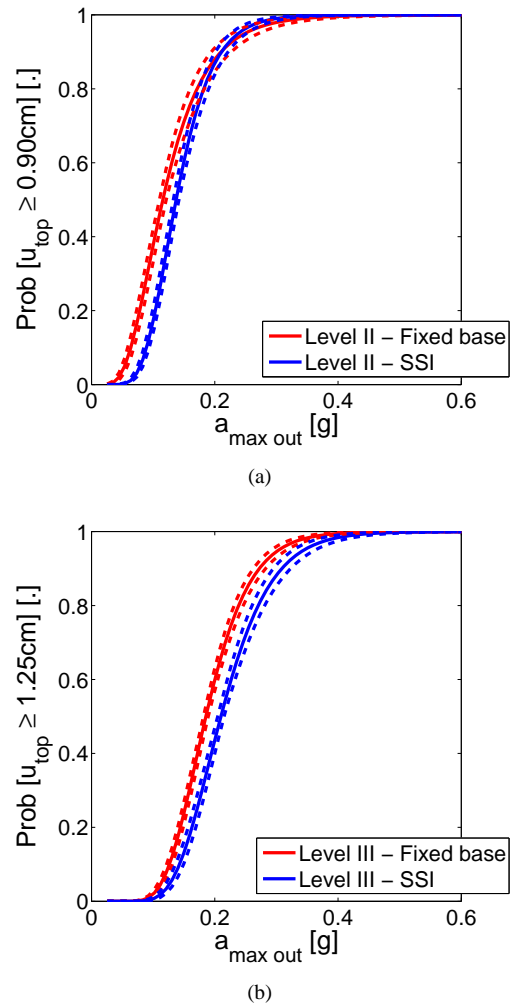


Figure 12. Comparison of fragility curves as a function of base condition. a) Level II (Moderate damage) and b) Level III (Extensive damage).

5 CONCLUSIONS

A series of finite element parametric analyses were used to investigate the effects to take into account the non-linear soil structure interaction on the response of infilled frame structures. A typical soil-structure model has been used to illustrate key results from parametric studies. According to the responses obtained with the model and for the particular case considered in this work (i.e. soil and structure model parameters), it can be concluded that:

- The inelastic analysis of the system under divers input motions shows the influence of the input signal on the structural and soil response;
- The addition of the non linear soil structure interaction affects the structure’s response. The structural drift obtained when the SSI is taken into account is higher than when it is neglected;
- The addition of the non linear SSI has an incidence on fragility curves obtained for this masonry infilled frame. A lower probability of damage is found;

- According to the comparison of the responses obtained in free field condition, it is observed that the earthquake motion at the structure's base is modified by the presence of the soil, in both acceleration level and frequency content;
- The main conclusion of this study is that the soil-structure interaction with a non-linear soil model varies significantly the response of the structure with respect to approximative SSI considerations. Further investigations in this way will be need in order to obtain more general conclusions for diverse structure and soil typologies.

ACKNOWLEDGMENTS

This study has been done in the framework of the French project ANR-07-PGCU-002, EVSIM - *Une approche mécanique d'Evaluation de la Vulnérabilité Sismique des Maçonneries.*

REFERENCES

- [1] ATC 40, "Seismic evaluation and retrofit of concrete buildings," Report atc, Applied Technology Council, 1996.
- [2] FEMA 356, "Prestandard and commentary for the seismic rehabilitation of buildings," Report FEMA, Federal Emergency Management Agency, 2000.
- [3] FEMA 440, "Improvement of nonlinear static seismic analysis procedures (draft)," Report ATC and FEMA, Applied Technology Council (ATC-55 Project) and Federal Emergency Management Agency, 2004.
- [4] D. Aubry, J.-C. Hujeux, F. Lassoudière, and Y. Meimon, "A double memory model with multiple mechanisms for cyclic soil behaviour," in *Int. Symp. Num. Mod. Geomech.* 1982, pp. 3–13, Balkema.
- [5] J.-C. Hujeux, "Une loi de comportement pour le chargement cyclique des sols," in *Génie Parasismique*. 1985, pp. 278–302, V. Davidovici, Presses ENPC, France.
- [6] D. Aubry, D. Chouvet, A. Modaressi, and H. Modaressi, "GEFDYN: Logiciel d'Analyse de Comportement Mécanique des Sols par Eléments Finis avec Prise en Compte du Couplage Sol-Eau-Air," Manuel scientifique, Ecole Centrale Paris, LMSS-Mat, 1986.
- [7] E. Saez, *Dynamic non-linear Soil-Structure Interaction*, PhD thesis, École Centrale Paris, France, 2009.
- [8] M. G. Katona and O. C. Zienkiewicz, "A unified set of single step algorithms part 3: the beta-m method, a generalization of the newmark scheme," *International Journal of Numerical Methods in Engineering*, vol. 21, no. 7, pp. 1345–1359, 1985.
- [9] H. Modaressi and I. Benzenati, "Paraxial approximation for poroelastic media," *Soil Dynamics and Earthquake Engineering*, vol. 13, no. 2, pp. 117–129, 1994.
- [10] M. Giberson, "Two nonlinear beams with definitions of ductility," *Journal of Structural Division, ASCE*, vol. 95, no. 2, pp. 137–157, 1969.
- [11] V. Prakash, G.H. Powel, and S. Campbell, *DRAIN 2D-X, Base program description and User Guide*, 1993.
- [12] M. Puglisi, M. Uzcatogui, and J. Florez-Lopez, "Modeling of masonry of infilled frames, Part I: The plastic concentrator," *Engineering Structures*, vol. 31, no. 1, pp. 113–118, 2009.
- [13] I. Doudoumis and E. Mitsopoulou, "Non-linear analysis of multistorey infilled frames for unilateral contact conditions," in *Proceedings of the eighth European conference on earthquake engineering, Lisbon*, 1986, vol. 3, pp. 6.5/63–70.
- [14] F. Lopez-Caballero and A. Modaressi-Farahmand-Razavi, "Numerical simulation of liquefaction effects on seismic SSI," *Soil Dynamics and Earthquake Engineering*, vol. 28, no. 2, pp. 85–98, 2008.
- [15] T. Iwasaki, F. Tatsuoka, and Y. Takagi, "Shear moduli of sands under cyclic torsional shear loading," *Soils and Foundations*, vol. 18, no. 1, pp. 39–56, 1978.
- [16] R. A. Medina and H. Krawinkler, "Seismic demands for nondeteriorating frame structures and their dependence on ground motions," Report No 144, John A. Blume Earthquake Engineering Center, Department of Civil and Environmental Engineering, Stanford University, 2003.
- [17] I. Iervolino and C. A. Cornell, "Record selection for nonlinear seismic analysis of structures," *Earthquake Spectra*, vol. 21, no. 3, pp. 685–713, 2005.
- [18] L. Sorrentino, S. Kunnath, G. Monti, and G. Scalora, "Seismically induced one-sided rocking response of unreinforced masonry façades," *Engineering Structures*, vol. 30, no. 8, pp. 2140–2153, 2008.
- [19] B.A. Bradley, R.P. Dhakal, G.A. MacRae, and M. Cubrinovski, "Prediction of spatially distributed seismic demands in specific structures: Ground motion and structural response," *Earthquake Engineering and Structural Dynamics*, vol. 39, no. 5, pp. 501–520, 2010.
- [20] A. Arias, "A mesure of earthquake intensity," in *Seismic Design for Nuclear Power Plants*. 1970, pp. 438–483, R.J. Hansen (ed.), MIT Press, Cambridge, Massachusetts.
- [21] E. M. Rathje, N. A. Abrahamson, and J. D. Bray, "Simplified frequency content estimates of earthquake ground motions," *Journal of Geotechnical and Geoenvironmental Engineering*, vol. 124, no. 2, pp. 150–159, 1998.
- [22] S. Koutsourelakis, J. H. Prévost, and G. Deodatis, "Risk assessment of an interacting structure-soil system due to liquefaction," *Earthquake Engineering and Structural Dynamics*, vol. 31, no. 4, pp. 851–879, 2002.
- [23] E. Cosenza, G. Manfredi, and R. Ramasco, "The use of damage functionals in earthquake engineering: A comparison between different methods," *Earthquake Engineering and Structural Dynamics*, vol. 22, no. 10, pp. 855–868, 1993.
- [24] E. Sáez, Fernando Lopez-Caballero, and A. Modaressi-Farahmand-Razavi, "Effect of the inelastic dynamic soil-structure interaction on the seismic vulnerability assessment," *Structural Safety*, vol. 33, no. 1, pp. 51–63, 2011.
- [25] J. C. Helton, J. D. Johnson, C. J. Sallaberry, and C. B. Storlie, "Survey of sampling-based methods for uncertainty and sensitivity analysis," *Reliability Engineering and System Safety*, vol. 91, no. 9-10, pp. 1175–1209, 2006.
- [26] W. Fellin, J. King, A. Kirsch, and M. Oberguggenberger, "Uncertainty modelling and sensitivity analysis of tunnel face stability," *Structural Safety*, vol. 32, no. 6, pp. 402–410, 2010.
- [27] M. Shinozuka, Q. Feng, J. Lee, and T. Naganuma, "Statistical analysis of fragility curves," *Journal of Engineering Mechanics - ASCE*, vol. 126, no. 12, pp. 1224–1231, 2000.
- [28] A. Penna, S. Cattari, A. Galasco, and S. Lagomarsino, "Seismic assessment of masonry structures by non-linear macro-element analysis," in *IV International Seminar on Structural Analysis of Historical Construction-Possibilities of Numerical and Experimental Techniques, Padova*, 2004, vol. 2, pp. 1157–1164.